Title
An automated behavioral box to assess forelimb function in rats

Authors
Wong, Chelsea C
Ramanathan, Dhakshin S
Gulati, Tanuj
et al.

Publication Date
2015-05-01

DOI
10.1016/j.jneumeth.2015.03.008

Peer reviewed

HHS Public Access

Author manuscript

J Neurosci Methods. Author manuscript; available in PMC 2017 June 15.

Published in final edited form as:

J Neurosci Methods. 2015 May 15; 246: 30–37. doi:10.1016/j.jneumeth.2015.03.008.

An automated behavioral box to assess forelimb function in rats

Chelsea C. Wong[1,2], **Dhakshin S. Ramanathan**[1,3,4], **Tanuj Gulati**[1,2], **Seok Joon Won**[1,2], and **Karunesh Ganguly**[1,2,*]

[1]Neurology & Rehabilitation Service, San Francisco VA Medical Center

[2]Department of Neurology, University of California, San Francisco

[3]Psychiatry Service, San Francisco VA Medical Center

[4]Department of Psychiatry, University of California, San Francisco

Abstract

Background—Rodent forelimb reaching behaviors are commonly assessed using a single-pellet reach-to-grasp task. While the task is widely recognized as a very sensitive measure of distal limb function, it is also known to be very labor-intensive, both for initial training and the daily assessment of function.

New Method—Using components developed by open-source electronics platforms, we have designed and tested a low-cost automated behavioral box to measure forelimb function in rats. Our apparatus, made primarily of acrylic, was equipped with multiple sensors to control the duration and difficulty of the task, detect reach outcomes, and dispense pellets. Our control software, developed in MATLAB, was also used to control a camera in order to capture and process video during reaches. Importantly, such processing could monitor task performance in near real-time.

Results—We further demonstrate that the automated apparatus can be used to expedite skill acquisition, thereby increasing throughput as well as facilitating studies of early versus late motor learning. The setup is also readily compatible with chronic electrophysiological monitoring.

Comparison with Existing Methods—Compared to a previous version of this task, our setup provides a more efficient method to train and test rodents for studies of motor learning and recovery of function after stroke. The unbiased delivery of behavioral cues and outcomes also facilitates electrophysiological studies.

Conclusions—In summary, our automated behavioral box will allow high-throughput and efficient monitoring of rat forelimb function in both healthy and injured animals.

1. Introduction

Rodent forelimb function is widely studied in the context of motor learning, neural plasticity and recovery from injury (Girgis et al., 2007; Hays et al., 2013; Kleim et al., 2007; Montoya et al., 1991; Ramanathan et al., 2006; Ramanathan et al., 2009; Rioult-Pedotti et al., 1998; Slutzky et al., 2010; Weishaupt et al., 2013; Whishaw et al., 2008; Whishaw et al., 1986).

*Corresponding author: karunesh.ganguly@ucsf.edu, 1700 Owens Street, Rm. 479, San Francisco, CA 94158, Phone: (415) 575-0401, Fax: (415) 750-2273.

More specifically, the Whishaw single-pellet reach-to-grasp task is among the mostly commonly used behavioral assessment of forelimb function (Fu et al., 2012; Kleim et al., 2007; Rioult-Pedotti et al., 1998; Whishaw et al., 2008; Whishaw et al., 1986; Whishaw and Pellis, 1990; Xu et al., 2009). Early variations of this task included the use of trays in the home cage containing multiple pellets simultaneously (Castro, 1972; Whishaw et al., 1986). The single-pellet task is more difficult as it requires reaching, grasping and retrieving a single pellet located at a distance outside of the behavior box (Whishaw and Pellis, 1990); inaccurate reaches typically result in the pellet being knocked away. The original version of this task included an acrylic box that biased reaching movements to a single limb and allowed video based monitoring of movements from multiple perspectives. Numerous studies have now shown that the single-pellet reaching task involves the learning and acquisition of a new motor skill (Conner et al., 2003; Francis and Song, 2011; Kleim et al., 2007; Rioult-Pedotti et al., 2000; Rioult-Pedotti et al., 1998); it has become an important focus for studies of the neural substrates of motor learning in both rats and mice (Fu et al., 2012; Kleim et al., 1998; Xu et al., 2009). The same task is also commonly used to study recovery of forelimb function after stroke or brain injury (Ramanathan et al., 2006; Whishaw et al., 2008; Whishaw et al., 1986). In addition, it may be used to assess motor function in other models of neurological dysfunction (e.g. Parkinson's disease) (Klein and Dunnett, 2012; Vergara-Aragon et al., 2003).

While the single-pellet reaching task is widely recognized as a very sensitive measure of distal forelimb function, it is also known to be very labor and time intensive (Kleim et al., 2007). In a typical reaching session, rats are given the opportunity to obtain 20–25 pellets (i.e. 20–25 trials per day). Traditionally, this requires an experimenter to manually present each pellet and to observe/shape the behavior of the rat by placing a subsequent pellet only when the rat has relocated to the other end of the cage. Such a training paradigm requires ~2 weeks to achieve adequate plateau performance levels (Francis and Song, 2011; Kleim et al., 2007). This is only compounded by the fact that multiple trials are necessary to assess outcomes after injury (i.e. if also used as a serial measure of functional recovery).

The primary goal of this study was to develop and validate a low-cost, automated high-throughput version of this task. Our specific focus was to minimize the need for user input and supervision during the training and assessment of animals. Importantly, the ability to automate assessments has the added benefit of facilitating blinding of assessments (i.e. done automatically without human intervention). We further demonstrated the potential use of such a box in varying the trial structure during motor learning as well as its compatibility with chronic electrophysiological recording techniques.

2. Methods

2.1 Subjects

We used a total of 22 male Long Evans rats weighing approximately 250 g. The rats were housed in a temperature-controlled, 12:12h light cycle environment in which behavioral testing occurred with lights on during the day. Rats were food scheduled, where they received a part of their food requirements from the reaching task depending on trial structure. Rats following the traditional training paradigm of one 25-trial session per day

were given an opportunity to obtain a maximum of 25 pellets in the behavior box, which made up approximately ~1/5 of their daily food intake. They were supplemented with 2 larger ‘rodent diet’ pellets (2500–3000mg each; 8640 Tklad 22/5 Rodent Diet, Harlan Laboratories, Indianapolis, IN) in their home cages after task performance. Rats undergoing high-throughput training paradigms obtained food ad lib during the task, which amounted to approximately ~2/3 of their daily intake, and were supplemented accordingly at the end of daily training. We measured body weight on a daily basis to ensure that their weight did not fall below 90% of their initial weight. Rats had free access to water when they were not performing the pellet reaching task. All housing and procedures were approved by the Institutional Animal Care and Use Committee at the San Francisco VA Medical Center (Animal Welfare Assurance Number A3476-01).

2.2 Apparatus

The reach box was made of acrylic sheets (250 x 300 x 200 mm, 3.175 mm thick [1/8”]; Acrycast, Calsak Plastics, Chino Hills, CA) and constructed with a central 12 mm wide slit in the front (Fig. 1). The centralized position and size of the slit only allowed access using one paw. The two “pellet trays” had a circumference of 7 mm with a 1 mm central depression (Supplementary Fig. 1) and were placed 15 mm in front of the slit and slightly left/right of center, respectively (Fig. 1A, F). The centers of the pellet trays were aligned with each respective edge of the central slit (Fig. 1A). Pellets were dispensed through flexible tubes (silicon tubing with 6.35 mm [1/4"] inner diameter, VetEquip Inc., Pleasanton, CA) (Fig. 1D). The tubing was attached to a front gate that controlled the opening of the slit (Fig. 1A, D). During the inter-trial period, the gate moved down to close the slit; a pellet was dispensed to the appropriate tray. During the following trial period, the gate moved up to allow access to the pellet (Fig. 1E, F).

Both a custom-built pellet dispenser (Fig. 1D, Supplementary Fig. 2) and a commercially available dispenser (Supplementary Fig. 3; Pellet Dispenser with 45mg Interchangeable Pellet Size Wheel, Lafayette Instrument Company, Lafayette, IN) were tested. The custom-built dispenser consisted of two tubes for pellet placement to either the left or the right tray (or to both simultaneously), which allowed for automatic determination of paw preference. This dispenser consisted of a clear acrylic tube (44.45 mm [1.75”] inner diameter, 4.76 mm [0.1875”] thick, and 63.5 mm [2.5”] height, Small Parts, Logansport, IN) attached with plastic bonder epoxy (Loctite, Westlake, OH) to an acrylic square bottom (63.5 mm x 63.5 mm [2.5” x 2.5”], 4.76 mm [0.1875”] thick). A 12.7 mm [0.5”] diameter hole was created in the center of the tube/bottom (Supplementary Fig. 1C). The shaft of a stepper motor (Hitec 32645S HS-645MG High Torque, HITEC RCD USA, Inc., Poway, CA) was inserted through the 12.7 mm [0.5”] hole and fixed using epoxy; a 44.45 mm [1.75”] circular plastic motor horn was then pushed to the bottom of the acrylic tube and attached to the stepper motor itself; the horn could then freely rotate. Two 6.35 mm [0.25”] holes were created in both the disc and the plastic bottom; the silicon tubes were attached to the plastic bottom such that when the holes were physically aligned, a pellet dropped through the respective tube onto either the L (left) or R (right) pellet tray (Fig. 1E). The customized dispenser required calibration in order to prevent crushing of the 45 mg pellets (45 mg dustless precision pellet, BioServ, Frenchtown, NJ). In contrast, the commercially available dispenser

was readily adapted without any further modifications. With the commercial dispenser, we were only able to deliver a pellet to either the L or R (i.e. required a physical switch of the silicon tubing). Notably, the use of two such dispensers can be used to replicate the two simultaneous outputs achieved using the customized dispenser.

An acrylic sheet gate was placed between the pellet tray and the slit (Fig. 1A, C, E). The dispenser tubes were attached to the gate itself. A second stepper motor (Hitec 32645S HS-645MG High Torque, HITEC RCD USA, Inc., Poway, CA) was used to control the position of the gate; gate opening was used to indicate the start of a trial and to allow access to the pellet trays. Pairs of infrared (IR) LED emitters (Sharp Microelectronics, Camas, WA) and IR detectors (Sharp Microelectronics, Camas, WA) were used to both detect the pellet on the tray (Fig. 1D, F) and the location of the rat between trials (Fig. 1B, C). An Arduino board (Arduino Uno - R3, Arduino, Ivrea, Italy) and motor shield (Arduino, Ivrea, Italy) were used to control both stepper motors described above. The IR emitter and the detector pairs were also monitored using the same board.

Dropped pellets were collected underneath the pellet trays and gate. A ramp ~15° from the horizontal allowed dropped pellets to roll down for collection in a receptacle placed at the base of the ramp. The ramp not only served to direct pellets into the receptacle but also to accentuate the motion of pellets as they traveled downward for detection as unsuccessful trials by the image processing system.

2.3 Computer control of the behavioral box

Control of the behavioral tasks, the stepper motors, monitoring of the IR sensors and video camera acquisition/monitoring was performed using custom built routines in MATLAB (MathWorks, Natick, MA). We have also developed a Graphical User Interface (GUI) that can readily control behavioral parameters, program modes, camera functions, and calibration (Supplementary Fig. 4). Drivers for the Arduino boards were downloaded from mathworks.com (http://www.mathworks.com/hardware-support/arduino-matlab.html). Our customized routines allowed us to easily modify the task structure, monitor the task performance during the task as well as to track overall performance in near real-time. Moreover, the trial data was saved in formats that could be easily opened in MATLAB or in Excel for further analysis.

2.4 Image processing based detection of trial outcomes

The behavioral apparatus was equipped with a laterally placed camera to monitor behavioral outcomes online (i.e. during the task performance) as well as to reconstruct limb kinematics offline. After each trial, the video was automatically processed in order to detect several parameters (Fig. 2A). First, the video was used to ensure that a pellet was truly dispensed. While pellets relatively infrequently failed to dispense (i.e. <2.5% of the time), such tracking ensured accurate performance characteristics. Specifically, a baseline image was taken during the box calibration step when no pellet is present. This was subtracted from the first frame of each acquired video clip. Accurate assessment of the pellet dispense was performed after conversion to a black and white image and measurement of the pixels in a region of interest (ROI) restricted to the expected location of the pellet. We found that this method

always detected the lack of a pellet drop (i.e. 100% accuracy). Such trials were then ignored and another pellet was dispensed. If a pellet successfully dropped onto the pellet tray, subsequent processing examined for the presence of a pellet in the ROI below the pellet trays (Fig. 2A, red outline). This ROI was examined to assess if a pellet had moved within it after being knocked off the pellet tray (unsuccessful trial) or if no pellet had slid down (in the case of a successful grasp and successful trial). The image based processing method (Fig. 2A) detected trial outcomes (i.e. 'dropped' or 'eaten') with an accuracy of 92 ± 4% (s.d., measurements conducted on n=10 reaching sessions consisting of 25 trials). Importantly, a ramp placed under the pellet trays (i.e. Fig. 2A), ensured that all dropped pellets moved through the ROI. Moreover, our behavioral testing was conducted in a soundproof chamber with controlled lighting. Stability of the background and the lighting conditions significantly improved the accuracy of the image processing. All trial videos were saved and could be reviewed offline in order to achieve complete accuracy of outcomes. These methods allowed us to detect sequences of trial outcomes in near real-time (Fig. 2B). As rats trained on the task, the frequency of successful outcomes increased, particularly toward the mid- to late- period of a 25-trial session.

For animals recovering from a stroke, we slightly modified the algorithm noted above; animals with significant forelimb deficits after stroke often moved the pellet (i.e. tripped the IR sensor) without actually dropping it. We thus added a step to ensure that the pellet had truly dropped (i.e. pushed off the pellet tray and not simply moved transiently). Specifically, we compared the last frame prior to complete gate closure to a baseline image without the pellet in place. Simple image subtraction allowed to us determine whether the pellet had truly dropped or was simply transiently displaced.

2.5 Behavioral training

All rats were given at least two days to acclimate to a restricted diet and the behavioral testing environment before task training began. There was no user intervention during this period. We have tested two approaches regarding the initial training. In the first, we started the reaching program in which the gate simply opened and remained open until the rats attempted to reach. In this completely unsupervised approach, we found that only a distinct minority of rats started to reach. Instead, consistent with past studies, an initial phase of training consisting of shaping the animals to understand the food pellet reward by olfactory familiarization was considerably better. We have successfully tested two possible approaches. In the first, the automatic setup was used to shape the rat. We placed an adaptor on top of the two pellet trays. This adaptor allowed the pellet to be dropped such that it was placed right at the slit (i.e. ~0.5 cm away), where the rats are able to lick the pellet. After 10–20 such trials, we switched to a "bilateral mode"; pellets are placed on both trays (Fig. 1F). The program automatically determines preference by examining which pellet is consistently dropped. After 10 trials, we then switched to the preferred side for continued training. A "manual mode" was also successfully tested. Thus, the experimenter manually placed pellets into the box through the slit to encourage rats to explore the front of the box. As rats gradually associated the slit with the delivery of reward, pellets were moved to the trays outside of the box and the automated training was engaged.

During the training phase, a reach attempt was deemed successful if the animal grasped for the pellet on the tray and brought it back into the box within the time frame of one trial. This time frame started with as much time as the rat needed to obtain the pellet and was gradually reduced to a 6 s window. The task was made increasingly more difficult by enforcing a hold period to trigger the start of a trial. A light sensor in the back of the box detected the presence of the rat before a trial could be initiated. The results outlined in the Results section involved a 6 s reaching window and did not require a hold period on Day 1. On subsequent days a hold period was instituted. Typically a rat was able to incorporate this feature quite easily.

For the single-session training paradigm, the rats had the opportunity to perform 25 trials/day. For the first multiple sessions per day training, animals could perform multiple 25 trial sessions separated by a 30 minute break (~10 sessions, ~250 trials). For the second version, animals could perform 100 trials/session (2–3x per day).

2.6 Stroke Induction

Unilateral lesion of the primary motor cortex (M1) was performed on n=4 rats using fiber optic illumination of Rose Bengal dye (Hsu and Jones, 2006; Watson et al., 1985; Whishaw et al., 1986). The optic-fiber cable was attached to the top of a 3 mm “induction tube” placed over the dura. The center of the tube was positioned over the center of the M1 region (2.5 mm lateral and 1 mm anterior to bregma). After femoral vein canalization and Rose Bengal infusion, a Polychrome fiber-optic source (KL 1200, Schott, Elmsford, NY) was used to illuminate the region for 20 minutes. Histological analysis (cresyl violet stain) was used to confirm the size and location of the resulting infarct.

2.7 Electrophysiology and Surgical Implantation

After performance of the reach task plateaued, three rats underwent a surgical procedure to implant recording electrodes (ZIF-Clip based 32-channel microwire arrays, Tucker-Davis Technologies, Alachua, FL) in M1 (Gulati et al., 2014). Rats were anesthetized with isoflurane at 1–3% and given atropine sulfate (0.02 mg/ kg b.w.) at the beginning of the surgery. After securing the animal in a stereotaxic frame (David Kopf Instruments, Tujunga, CA), a craniotomy was performed over the forelimb motor area with dimensions 6 mm to -2 mm anteroposterior and 1 mm to 5 mm mediolateral from bregma. Arrays were lowered to a depth of 1,400–1,800 μm in the forelimb area (1–3 mm anterior to bregma and 2–4 mm lateral from midline), where the dura mater was retracted. Final localization of the array was based on quality of recordings across channels at the time of implantation. The reference and ground wires of the array were wrapped around screws placed in the skull region over the cerebellum to ensure minimal noise in electrophysiology recordings. The postoperative recovery regimen included administration of buprenorphine at 0.02 mg/kg b.w. and meloxicam at 0.2 mg/kg b.w. Dexamethasone at 0.5 mg/kg b.w. and trimethoprim sulfadiazine at 15 mg/kg b.w. were also administered post-operatively for 5 days. All animals were given at least 5 days to recover before the start of experiments.

We recorded spike and LFP activity using a 128–channel TDT–RZ2 system (Tucker–Davies Technologies, Alachua, FL). Spike data was sampled at 24414 Hz and LFP data at 1018 Hz.

ZIF–clip based analog headstages with a unity gain and high impedance (~1 GΩ) were used. Only clearly identifiable units with good waveforms and high signal–to–noise were used. The remaining neural data was recorded for offline analysis. We sorted the MEA recordings using standard offline cluster cutting methods in TDT's OpenSorter software. Behavior related timestamps (i.e. trial onset, trial completion) were sent to the RZ2 analog input channel using an Arduino digital board and synchronized to neural data.

2.8 Statistical analysis

We performed one-way ANOVA with multiple comparisons for significance assessment of plateau success rates for different training paradigms (MATLAB, MathWorks, Natick, MA).

3. Results

3.1 Traditional and high-throughput training paradigms

We systematically varied the trial structure and exposure to the task in order to test the time-dependent differences in motor skill formation. Traditionally, one training session of 25 trials per day prepared naïve rats to understand the task reward structure and gradually master the reaching technique over two to three weeks (Fig. 3A). The automation of the setup enabled us to train multiple rats simultaneously in closed, soundproof chambers. The independent, self-regulating nature of the apparatus further prompted the implementation of high-throughput training paradigms, which yielded multiple sessions per day. Two additional protocols were tested: ~10 sessions of 25 trials each day (Fig. 3B) and 2–3 sessions of 100 trials each day (Fig. 3C). Both methods expedited the time to task plateau without significant differences in the final absolute success rate (plateau success rates: 66.9 ± 3.9%, n=6 animals; 74.5 ± 3.4%, n=8; and 60.5 ± 4.8%, n=4 respectively for one 25 trial session per day, multiple sessions of 25 trials each per day and multiple 100 trial sessions per day, respectively, mean ± s.e.m., *one-way* ANOVA, $F_{2,33} = 3.09$; $P > 0.05$).

3.2 Learning and recovery after stroke

We also verified that rats trained using the high-through method experienced a similar recovery after stroke; we wanted to ensure that there is no fundamental difference in skill acquisition relative to rats trained using a more traditional time window. After animals achieved a stable performance rate, they underwent a unilateral photothrombotic stroke to the contralateral primary motor cortex (Fig. 4). The injury consistently damaged forelimb function in the reaching paw; all rats were unable to reach initially during one traditional testing session following the post-operative regimen. We observed a slow recovery of motor function that resembled previously published data (Gharbawie et al., 2005; Ramanathan et al., 2006).

3.3 Compatibility with electrophysiology

While reaching tasks have been studied using cellular and molecular techniques, less is known about the electrophysiological basis of skilled motor learning in awake-behaving animals. We wanted to also demonstrate that the automated reaching box is ideally suited for electrophysiological investigations. We time-locked the behavioral, video and neural data in two ways: (1) by syncing neural data to the frame rate of the video of actual movements (i.e.

MATLAB sent simultaneous triggers to the electrophysiology workstation and the video camera) and (2) using the IR sensor embedded under the pellet tray as a marker for a pellet drop. The embedded sensors allowed us to modify the trial structure easily and to incorporate a hold period (Fig. 5A). Figure 5 shows an example of a M1 neuron that is active mid-way through the each period (Fig. 5A–C). In general, we found that M1 neurons were active throughout the reach phase (Fig. 5D). Consistent with past data, we found that the majority of M1 neural neurons were most active after the onset of reach. It is likely that our recording location, which targeted the distal forelimb region (Hyland, 1998; Peters et al., 2014), contributed to the activation profile. Thus, during a reach-and-grasp task, the majority of activity in M1 at this location appeared to be related to grasping.

DISCUSSION

The single-pellet reaching task is a validated method to evaluate forelimb function in rats (Francis and Song, 2011; Kleim et al., 2007). However, the necessity for manual placement of pellets and determination of trial outcomes is a significant burden, both with respect to time invested as well as a possible confound during electrophysiological assessments. Our results illustrate the feasibility of fashioning a low-cost automated behavioral setup that permits high-throughput training and assessment. The automated nature of the setup allowed us to systematically vary the trial structure during the skill acquisition phase. As a proof-of-principle, we found that by significantly increasing the trials per session we could reliably achieve plateau performance over 3–4 days, representing a significant reduction in the training period. We further show that the rapid acquisition of skill resulted in similar recovery schedules after focal stroke. Finally, we demonstrate that our behavioral box is readily compatible with chronic electrophysiological monitoring.

The automated behavioral box allowed us to quite easily modulate the trial structure during the initial skill acquisition phase. From a pragmatic perspective, by increasing either the number of sessions per day or the number of trials per session we were able to achieve plateau performance levels over a shorter interval. We did not find significant differences from the final performance levels of rats that were trained using the more traditional method of 20–25 trials per day. While this is not unexpected given the wealth of data on the role of practice on motor performance, it should facilitate study of the temporal course of motor learning (i.e. understanding the neural basis of early and late motor learning) (Costa et al., 2004; Francis and Song, 2011; Fu et al., 2012; Shmuelof and Krakauer, 2011). For example, current electrophysiological methods are unable to easily record the same neural ensemble over extended periods of time (Chestek et al., 2011; Suner et al., 2005). Reducing the learning process to a 1–3 day period of time should significantly facilitate endeavors to track learning and neural ensembles over extended periods of time (Ganguly and Carmena, 2009; Ganguly et al., 2011; Gulati et al., 2014).

We also used our automated single-pellet reaching box to assess recovery of motor function after stroke. We developed strategies to more accurately measure trial performance in post-ischemic lesion rats. For example, animals with significant forelimb deficits often moved the pellet (i.e. tripped the IR sensor) without actually dropping it. We thus added a step to ensure that the pellet had truly dropped prior to the image-processing step (i.e. Figure 2). We also

ensured that recovery after the expedited training was similar to that reported for more traditional training schedules. This suggests that a focal M1 stroke is able to similarly disrupt the reaching behavior regardless of the speed of skill acquisition (i.e. multiple sessions over a few days versus a single session per day over 2–3 weeks). Furthermore, video recording of trials allowed for detailed kinematic analysis of forelimb reach trajectories. We anticipate that our setup can also be used to easily and systematically vary the trial structure during recovery after stroke.

Conclusion

Our automated behavioral setup facilitates high-throughput training and assessment of forelimb function in rats without constant experimenter supervision. The modular apparatus is readily adaptable to customized task structures, allowing for numerous variations to be tested. By expediting the acquisition period for skilled reaching, the temporal evolution of motor learning can be more easily examined, particularly in correlation with electrophysiology recordings. Given its flexibility, the setup is also amenable to evaluating a wide spectrum of rodent models; for example, the effects of different forms of brain injury, age, hand preference and strain can be studied in an unbiased (i.e. blinded) manner. Based on our results, we anticipate that our design will provide a more efficient method to study forelimb function in rats (e.g. training, stable performance, sleep, recovery following traumatic brain injury).

Supplementary Material

Refer to Web version on PubMed Central for supplementary material.

Acknowledgments

This work was supported by the Department of Veterans Affairs (CDA-2B6674W), the Burroughs Wellcome Fund, the American Heart/Stroke Association (0875016N) and departmental funds from the UCSF Department of Neurology. We would also like to thank Roy Tangsombatvisit for assistance with the design and the manufacturing of the reach boxes.

References

Castro AJ. The effects of cortical ablations on digital usage in the rat. Brain Res. 1972; 37:173–85. [PubMed: 5061111]

Chestek CA, Gilja V, Nuyujukian P, Foster JD, Fan JM, Kaufman MT, Churchland MM, Rivera-Alvidrez Z, Cunningham JP, Ryu SI, Shenoy KV. Long-term stability of neural prosthetic control signals from silicon cortical arrays in rhesus macaque motor cortex. J Neural Eng. 2011; 8:045005. [PubMed: 21775782]

Conner JM, Culberson A, Packowski C, Chiba AA, Tuszynski MH. Lesions of the Basal forebrain cholinergic system impair task acquisition and abolish cortical plasticity associated with motor skill learning. Neuron. 2003; 38:819–29. [PubMed: 12797965]

Costa RM, Cohen D, Nicolelis MA. Differential corticostriatal plasticity during fast and slow motor skill learning in mice. Curr Biol. 2004; 14:1124–34. [PubMed: 15242609]

Francis JT, Song W. Neuroplasticity of the sensorimotor cortex during learning. Neural plasticity. 2011; 2011:310737. [PubMed: 21949908]

Fu M, Yu X, Lu J, Zuo Y. Repetitive motor learning induces coordinated formation of clustered dendritic spines in vivo. Nature. 2012; 483:92–5. [PubMed: 22343892]

Ganguly K, Carmena JM. Emergence of a stable cortical map for neuroprosthetic control. Plos Biol. 2009; 7:e1000153. [PubMed: 19621062]

Ganguly K, Dimitrov DF, Wallis JD, Carmena JM. Reversible large-scale modification of cortical networks during neuroprosthetic control. Nat Neurosci. 2011; 14:662–7. [PubMed: 21499255]

Gharbawie OA, Gonzalez CL, Williams PT, Kleim JA, Whishaw IQ. Middle cerebral artery (MCA) stroke produces dysfunction in adjacent motor cortex as detected by intracortical microstimulation in rats. Neuroscience. 2005; 130:601–10. [PubMed: 15590144]

Girgis J, Merrett D, Kirkland S, Metz GA, Verge V, Fouad K. Reaching training in rats with spinal cord injury promotes plasticity and task specific recovery. Brain. 2007; 130:2993–3003. [PubMed: 17928316]

Gulati T, Ramanathan DS, Wong CC, Ganguly K. Reactivation of emergent task-related ensembles during slow-wave sleep after neuroprosthetic learning. Nat Neurosci. 2014

Hays SA, Khodaparast N, Sloan AM, Hulsey DR, Pantoja M, Ruiz AD, Kilgard MP, Rennaker RL 2nd. The isometric pull task: a novel automated method for quantifying forelimb force generation in rats. J Neurosci Methods. 2013; 212:329–37. [PubMed: 23183016]

Hsu JE, Jones TA. Contralesional neural plasticity and functional changes in the less-affected forelimb after large and small cortical infarcts in rats. Exp Neurol. 2006; 201:479–94. [PubMed: 16797536]

Hyland B. Neural activity related to reaching and grasping in rostral and caudal regions of rat motor cortex. Behav Brain Res. 1998; 94:255–69. [PubMed: 9722277]

Kleim JA, Barbay S, Nudo RJ. Functional reorganization of the rat motor cortex following motor skill learning. J Neurophysiol. 1998; 80:3321–5. [PubMed: 9862925]

Kleim JA, Boychuk JA, Adkins DL. Rat models of upper extremity impairment in stroke. ILAR J. 2007; 48:374–84. [PubMed: 17712223]

Klein, A., Dunnett, SB. Analysis of skilled forelimb movement in rats: the single pellet reaching test and staircase test. In: Crawley, Jacqueline N., et al., editors. Current protocols in neuroscience / editorial board. Vol. Chapter 8. 2012. p. 28

Montoya CP, Campbell-Hope LJ, Pemberton KD, Dunnett SB. The "staircase test": a measure of independent forelimb reaching and grasping abilities in rats. J Neurosci Methods. 1991; 36:219–28. [PubMed: 2062117]

Peters AJ, Chen SX, Komiyama T. Emergence of reproducible spatiotemporal activity during motor learning. Nature. 2014; 510:263–7. [PubMed: 24805237]

Ramanathan D, Conner JM, Tuszynski MH. A form of motor cortical plasticity that correlates with recovery of function after brain injury. Proc Natl Acad Sci U S A. 2006; 103:11370–5. [PubMed: 16837575]

Ramanathan D, Tuszynski MH, Conner JM. The basal forebrain cholinergic system is required specifically for behaviorally mediated cortical map plasticity. J Neurosci. 2009; 29:5992–6000. [PubMed: 19420265]

Rioult-Pedotti MS, Friedman D, Donoghue JP. Learning-induced LTP in neocortex. Science. 2000; 290:533–6. [PubMed: 11039938]

Rioult-Pedotti MS, Friedman D, Hess G, Donoghue JP. Strengthening of horizontal cortical connections following skill learning. Nat Neurosci. 1998; 1:230–4. [PubMed: 10195148]

Shmuelof L, Krakauer JW. Are we ready for a natural history of motor learning? Neuron. 2011; 72:469–76. [PubMed: 22078506]

Slutzky MW, Jordan LR, Bauman MJ, Miller LE. A new rodent behavioral paradigm for studying forelimb movement. J Neurosci Methods. 2010; 192:228–32. [PubMed: 20691727]

Suner S, Fellows MR, Vargas-Irwin C, Nakata GK, Donoghue JP. Reliability of signals from a chronically implanted, silicon-based electrode array in non-human primate primary motor cortex. Ieee T Neur Sys Reh. 2005; 13:524–41.

Vergara-Aragon P, Gonzalez CL, Whishaw IQ. A novel skilled-reaching impairment in paw supination on the "good" side of the hemi-Parkinson rat improved with rehabilitation. J Neurosci. 2003; 23:579–86. [PubMed: 12533618]

Watson BD, Dietrich WD, Busto R, Wachtel MS, Ginsberg MD. Induction of reproducible brain infarction by photochemically initiated thrombosis. Ann Neurol. 1985; 17:497–504. [PubMed: 4004172]

Weishaupt N, Vavrek R, Fouad K. Training following unilateral cervical spinal cord injury in rats affects the contralesional forelimb. Neurosci Lett. 2013; 539:77–81. [PubMed: 23384567]

Whishaw IQ, Alaverdashvili M, Kolb B. The problem of relating plasticity and skilled reaching after motor cortex stroke in the rat. Behav Brain Res. 2008; 192:124–36. [PubMed: 18282620]

Whishaw IQ, O'Connor WT, Dunnett SB. The contributions of motor cortex, nigrostriatal dopamine and caudate-putamen to skilled forelimb use in the rat. Brain. 1986; 109 (Pt 5):805–43. [PubMed: 3779371]

Whishaw IQ, Pellis SM. The structure of skilled forelimb reaching in the rat: a proximally driven movement with a single distal rotatory component. Behav Brain Res. 1990; 41:49–59. [PubMed: 2073355]

Xu T, Yu X, Perlik AJ, Tobin WF, Zweig JA, Tennant K, Jones T, Zuo Y. Rapid formation and selective stabilization of synapses for enduring motor memories. Nature. 2009; 462:915–9. [PubMed: 19946267]

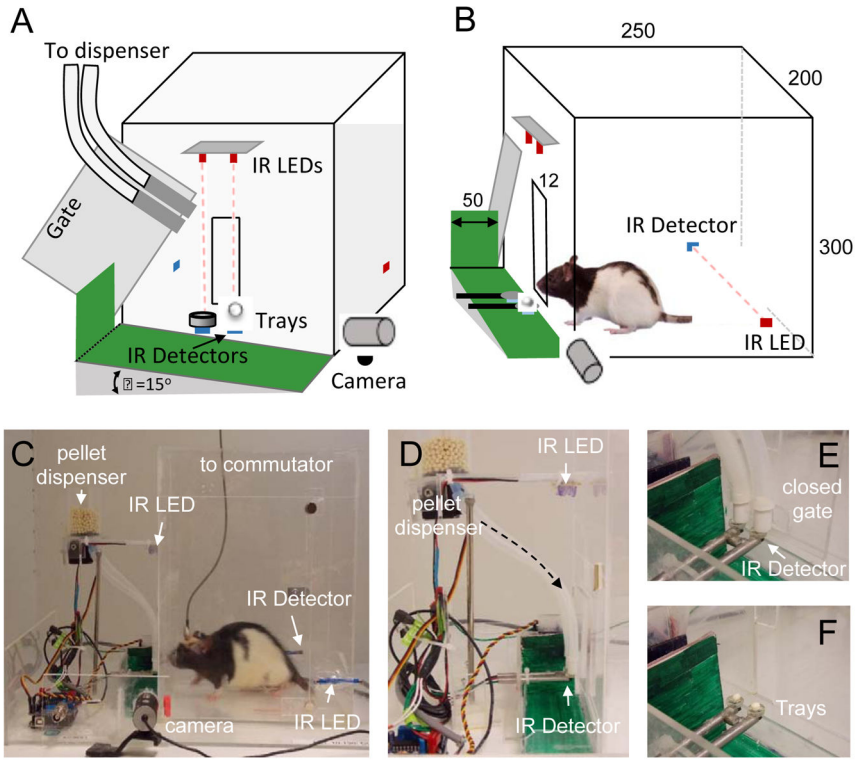

Figure 1. Behavioral apparatus

(A) Schematic drawing of the box with open gate. Red boxes represent the infrared (IR) light emitting diodes (LED); Blue boxes represent the IR detectors. Dashed lines indicate IR beams for pellet detection. (B) Schematic drawing of the side view of the box. (C) View of the entire reach box with pellet dispenser and gate-controlled slit on the left. (D) Customized dual-output pellet dispenser. Arrow indicates direction of pellet dispensing to left and right pellet trays. (E–F) Illustration of the dual pellet holders. With the gate closed, pellets can be easily dispensed to either the left or right position. Opening of the gate signals the start of the trial and presentation of the pellet.

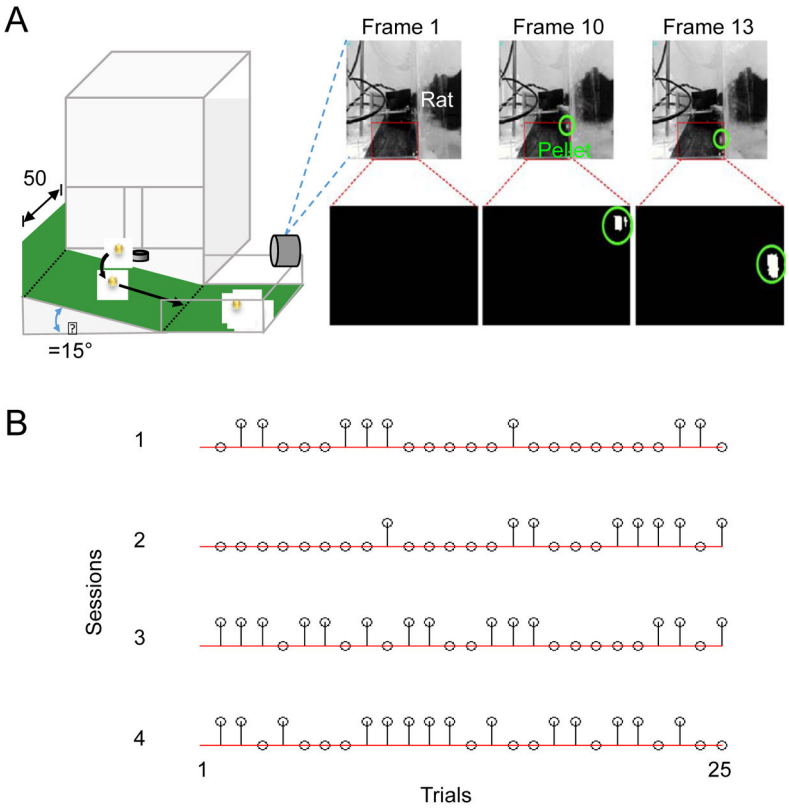

Figure 2. Automated detection of trial outcomes

(A) Examples of video processing to detect single trial outcomes. Image above is a black and white depiction of a single video frame (30 Hz acquisition). Region of interest (ROI) is indicated by the red rectangle. Shown below is the processed indication of a dropped pellet (i.e., the white pixels in frames 10 and 13). The pellets and the detected trajectory of the pellet are outlined in green. (B) Single trial outcomes during multiple learning sessions in a single day. Stems indicate successful trials, while circles on the red line indicate failures. Top row is the first training session of the day.

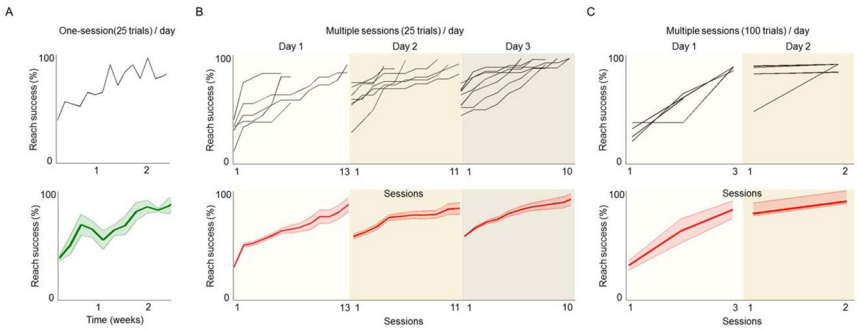

Figure 3. Comparison of trial structure on the reach-to-grasp task

(A) Upper panels show the learning curve of one rat during regular training paradigm of one 25-trial session per day. The lower panel shows the mean curve for 6 rats. (B) Upper panel shows multiple individual examples of multiple daily sessions per day (25 trials/session). Mean curve is shown below (n=8 rats). (C) Examples and mean for rats performing multiple sessions of 100 trials/session.

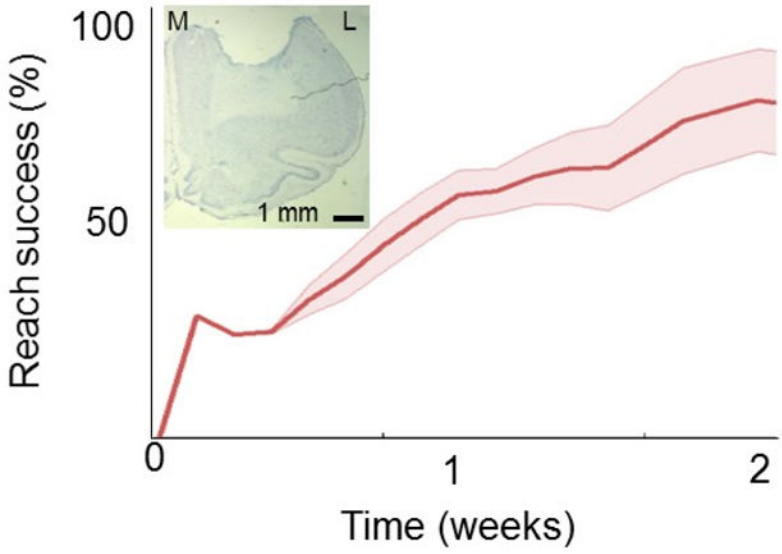

Figure 4. Recovery after stroke

Mean recovery curve after a focal M1 stroke (n=4). Each of these rats were trained using multiple sessions/day. The inset shows the histological analysis (cresyl violet stain) of the stroke from one animal (coronal section). Scale bar is 1 mm. M=Medial; L=Lateral.

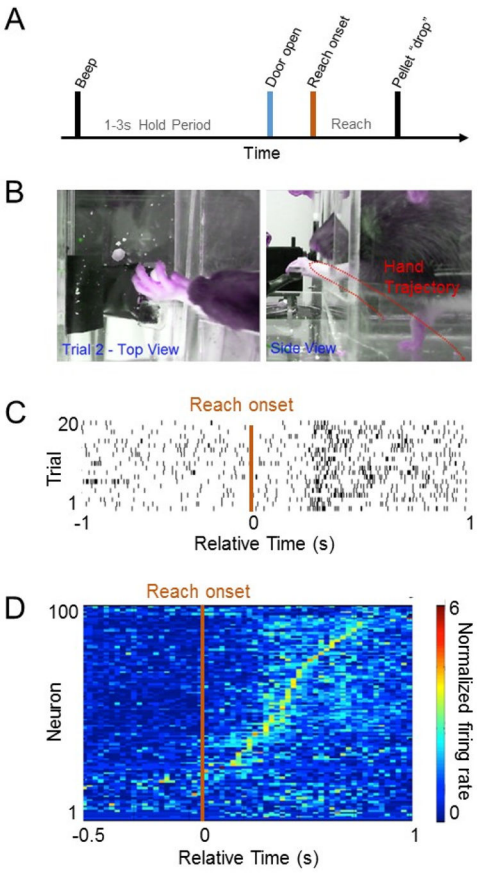

Figure 5. Electrophysiological recordings from the rat primary motor cortex (M1) during reaching

(A) Trial structure during reaching movements. (B) Still frames of video tracking of limb movements. The red line shows a single example of the reach trajectory. (C) Example firing of a single neuron in M1 during reaching movements. Each row represents activity during a single reaching movement and each bar represents an action potential/spike. (D) Colormap of the temporal evolution of the neural spiking activity during reaching movements (combined from recording sessions in three rats). Time 0 is the reach onset. Each row represents the mean normalized event-related firing of task-related neurons. Color gradient represents the normalized peak firing intensity (i.e. normalized firing rate).